Modulating L-Type Calcium Current Affects Discontinuous Cardiac Action Potential Conduction

Ronald W. Joyner,* Rajiv Kumar,* Ronald Wilders,#§ Habo J. Jongsma,# E. Etienne Verheijck,#§ David A. Golod,* Antoni C. G. van Ginneken,§ Mary B. Wagner,*¶ and William N. Goolsby*

*Todd Franklin Cardiac Research Laboratory, The Children's Heart Center, Department of Pediatrics, Emory University, Atlanta, Georgia 30322, USA; #Department of Medical Physiology and Sports Medicine, Utrecht University, 3584 CG Utrecht, The Netherlands; §Department of Physiology, University of Amsterdam, 1105 AZ Amsterdam, The Netherlands; and ¶Bioengineering Graduate Group, University of California, San Francisco, and University of California, Berkeley, California 94708 USA

ABSTRACT We have used pairs of cardiac cells (i.e., one real guinea pig ventricular cell and a real-time simulation of a numerical model of a guinea pig ventricular cell) to evaluate the effects on action potential conduction of a variable coupling conductance in combination with agents that either increase or decrease the magnitude of the L-type calcium current. For the cell pairs studied, we applied a direct repetitive stimulation to the real cell, making it the "leader" cell of the cell pair. We have demonstrated that significant delays in action potential conduction for a cell pair can occur either with a decreased value of coupling conductance or with an asymmetry in size such that the follower cell is larger than the leader cell. In both conditions we have shown that isoproterenol, applied to the real cell at very low concentrations, can reversibly decrease the critical coupling conductance (below which action potential conduction fails) for a cell pair with fixed cell sizes, or, for a fixed value of coupling conductance, increase the maximum allowable asymmetry in cell size for successful conduction. For either of these effects, we were able to show that treatment of the real cell with BayK 8644, which more specifically increases the magnitude of the L-type calcium current, was able to mimic the actions of isoproterenol. Treatment of the leader cell of the cell pair (the real cell) with nifedipine, which selectively lowers the magnitude of the L-type calcium current, had effects opposite those of isoproterenol or BayK 8644. The actions of nifedipine, isoproterenol, and BayK 8644 are all limited to conditions in which the conduction delay is on the order of 5 ms or more, whether this delay is caused by limited coupling conductance or by asymmetry in size of the cells. This limitation is consistent with the time course of the L-type calcium current and suggests that the effects of calcium channel blockers or β-adrenergic blocking drugs, in addition to being selective for regions of the heart that depend on the L-type calcium current for the upstroke of the action potential, would also be somewhat selective for regions of the heart that have discontinuous conduction, either normally or because of some pathological condition.

INTRODUCTION

Action potential conduction throughout the heart is known to be a process that shows large variations in direction and velocity of the propagating wavefront in different regions of the heart because of the spatial inhomogeneity of the distribution of both cellular membrane properties and gap junctions, which serve as low-resistance pathways for cell-to-cell current flow. We have used theoretical simulations (Joyner, 1986) and experimental studies with a "coupling clamp" circuit to investigate discontinuous conduction in pairs of isolated cardiac cells (Joyner et al., 1991; Sugiura and Joyner, 1992). We studied geometrical factors responsible for unidirectional block (Joyner et al., 1991) by deliberately choosing cells that were either similar in size or quite different in size (as measured quantitatively by the cell capacitance, the current threshold, and the reciprocal of the input resistance). In cell pairs of asymmetrical size we showed that bidirectional block occurred at low values of coupling conductance (G_c), that bidirectional conduction occurred at higher values of G_c, and that there was a "window" of G_c values over which unidirectional block occurred. Another interesting phenomenon also occurred in these experiments: during the conduction delay between the activation of the stimulated cell (leader cell) and delayed activation of the other cell (follower cell) there was a substantial partial repolarization of the leader cell, which then reversed quickly when the follower cell activated. We also noted that action potential peak amplitude and excitability of the leader cell were not affected by the electrical load that determined conduction failure or success. This suggested that the L-type calcium current (I_{Ca}) was much more important in the conduction process than previously considered, at least for cells with discontinuous conduction. We also did experiments (Sugiura and Joyner, 1992) in which we coupled pairs of isolated guinea pig (GP) ventricular cells over a wide range of G_c and compared the conduction delay and the extent of the partial repolarization of the leader cell in normal Tyrode's solution versus that observed for the same cell pairs with submaximum concentrations of nifedipine, a calcium channel blocker. We showed that the critical G_c (the value of G_c below which conduction block was produced) was increased significantly by nifedipine and that, at a given value of G_c, the conduc-

Received for publication 10 January 1996 and in final form 27 March 1996.

Address reprint requests to Dr. R. W. Joyner, Department of Pediatrics, Emory University, 2040 Ridgewood Dr. NE, Atlanta, GA 30322. Tel.: 404-727-5747; Fax: 404-727-6024; E-mail: rjoyner@anatomy.emory.edu.

0006-3495/96/07/237/09 $2.00

tion delay and the extent of the early repolarization were increased by nifedipine. The extent of the early repolarization in the leader cell also suggested that the actual magnitude of I_{Ca} that flowed during the action potential might be asymmetrical, with more I_{Ca} for the leader cell than for the follower cell because of differences in the early part of the action potential waveform. We confirmed this prediction (Kumar and Joyner, 1995) by using action potentials recorded from coupled cells (in current clamp mode) as time-varying command potentials for other cells in voltage clamp mode. We first simultaneously recorded action potentials from the leader cell (stimulated cell, cell 1) and the follower cell (nonstimulated cell, cell 2) of a cell pair, with a fixed G_c between the cells supplied by our coupling circuit. We then applied these recorded action potentials as command potential waveforms for other cells studied in the voltage clamp mode, for which we used internal and external solutions that isolated I_{Ca}. We showed that discontinuous conduction is associated with a directionally determined asymmetry in I_{Ca}, with the leader cell having a larger I_{Ca} than the follower cell, which may be significant in determining the success or failure of conduction.

There have been many published models of the cardiac action potential in single cardiac cells, from the Beeler-Reuter model (Beeler and Reuter, 1977) to the recent Luo and Rudy (LR) model (Luo and Rudy, 1994a,b). The increasing speed of available computers has now made it possible to solve these systems of differential equations in "real time" with a reasonable time step for integration. With an A/D and a D/A converter, the computer can thus produce an "interactive" model in which the solution of the model is coupled in real time by some desired G_c to a real cell from which recordings are being made in the current clamp mode. As shown in our recent publication (Wilders et al., 1996), when we coupled the LR model cell to a GP ventricular cell, we obtained action potential conduction either from the LR model cell to the real cell or from the real cell to the LR model cell, depending on which cell received direct stimulation and on the value of G_c. We emphasized in the Wilders et al. (1996) publication the effects of extreme uncoupling of cells. We have now extended this work to examine the consequences of variations of G_c over a wide range of values, variations in the relative size of the leader and the follower cell, and pharmacological modulation of the L-type calcium current of the leader cell of the cell pair. We have used a hybrid cell pair (one real cell and one model cell) for these experiments instead of a pair of real cells for several reasons. First, the cell model is entirely consistent and reproducible in every experiment, providing a standard "follower" cell with a constant current threshold. Second, experiments with a real cell coupled to a model cell require only one stable recording from a real cell, which is much easier than achieving two simultaneously stable recordings from real cells. Third, because we are using pharmacological modulation of L-type calcium current, we wanted to apply the drugs (and thus the pharmacological effects) only to the leader cell of the cell pair to specifically evaluate the role of the L-type calcium current of the leader cell in modulating action potential conduction for cell pairs.

MATERIALS AND METHODS

Isolation of ventricular cells

The enzymatic procedure for single cell isolation was similar to that previously described by Yazawa et al. (1990). Animals used include guinea pigs weighing 300–600 g. Each animal was anesthetized with 50 mg/kg nembutal i.p. The trachea was cannulated for artificial respiration during a thoracotomy, by which the heart was rapidly excised and the aorta was cannulated for Langendorff perfusion. The heart was first perfused for 3–5 min at a rate of 6–10 ml/min with normal Tyrode's solution. After the blood had been washed out of the coronary arteries, the heart was perfused with nominally Ca^{2+}-free Tyrode's solution for 5–6 min. For isolation of ventricular cells, the heart was then perfused with the nominally Ca^{2+}-free Tyrode solution containing collagenase (4–8 mg/100 ml; Yakult) and protease (type XIV, 1 mg/100 ml; Sigma) for 5–10 min. The enzymes were then washed out of the heart with a high-K^+/low-Cl^- storage solution for 5 min. After perfusion of the high-K^+ storage solution, both ventricles were cut into pieces and gently triturated in the high-K^+ storage solution and stored at 4°C. The isolated cells were transferred to an experimental chamber and continuously superfused with normal Tyrode's solution at 2 ml/min at 36–37°C. Only quiescent cells with preservation of their rod-shaped appearance were studied, using relatively high-resistance patch pipettes (4–6 MΩ) to minimize intracellular dialysis. The composition of solutions used was as follows (mM): normal Tyrode: NaCl 148.8, KCl 4, $CaCl_2$ 1.8, $MgCl_2$ 0.53, NaH_2PO_4 0.33, HEPES 5, dextrose 5, with pH adjusted to 7.4 using NaOH. Ca^{2+}-free Tyrode: NaCl 148.8, KCl 4, $MgCl_2$ 0.53, NaH_2PO_4 0.33, HEPES 5, dextrose 5, with pH adjusted to 7.4 using NaOH. Storage solution: potassium glutamate 120, taurine 20, $MgCl_2$ 5, EGTA 1, dextrose 10, HEPES 10, with pH adjusted to 7.4 using KOH. Pipette solution for current clamp recordings: KCl 145, Mg-ATP 5, Na_2 creatine phosphate 5.0, and HEPES 5.0, pH 7.2 with KOH. Nifedipine (Sigma) was dissolved in dimethyl sulfoxide to make a 20 mM stock solution, and isoproterenol was dissolved in 1 mM ascorbic acid solution to make a 1 mM stock solution. The stock solutions were diluted into normal Tyrode's solution to the desired final concentration.

Electrical coupling of a real GP ventricular cell to a cell model

We have developed an electrical circuit that can provide a variable effective G_c between two isolated heart cells that are not actually in direct contact with each other (Tan and Joyner, 1990; Joyner et al., 1991). The specification of G_c is a combination of the fixed gain of the voltage-to-current ("V to I") converters and the variable gain of the two amplifiers, giving us control of the G_c in our experiments. Current pulses of 2 ms duration and amplitude of 5–10% suprathreshold are applied to the stimulated cell at a frequency of 1–2 Hz. Simultaneous recordings from each cell are made with an Axoclamp 2A (Axon Instruments, Inc.) dual amplifier, using the internal V to I converters to feed back the desired currents to each headstage from the coupling circuit. The LR model for an isolated GP ventricular cell (Luo and Rudy, 1994a,b) includes sarcolemmal ionic channel currents and pump currents as well as a representation of calcium ion concentration with cytoplasmic buffers and the release and uptake of calcium by the sarcoplasmic reticulum. Throughout this paper we use this "LR 2" model and not the previously published "LR 1" model (Luo and Rudy, 1991). The LR cell model has a capacitance of 153.4 pF and an effective "input resistance" of about 20 MΩ for small depolarizations, thus having an input time constant of about 3 ms. The stimulus current threshold for this model is 2.6 nA for a stimulus duration of 2 ms. Because the LR model contains some components with fast kinetics, it is to be expected that the time step of 70 μs imposed by our computational hardware would have some effect on the model solution. We have done extensive testing to

evaluate how this discrete time step affects the solution of the LR model, showing that neither the excitability nor the action potential duration is affected by more than a few percent. These tests are included in our recent publication (Wilders et al., 1996).

Adjustments of the effective cell size for the leader or follower cell

The large variation in cell size (represented by variations in the current threshold for excitation) that is found experimentally represents an experimental problem but also an opportunity to study the effects of cell size on conduction properties. The inclusion in our coupling model of the ability to change the effective cell size of either the computer model and/or the real cell is necessary for normalization of the results. This capability is produced by simply scaling the coupling current that is being applied to either the real GP ventricular cell (cell 1) by Z_1 and the coupling current, which is being applied to the LR model cell (cell 2) by Z_2. This produces a time-varying coupling current equal to $Z_2 * (V_1 - V_2) * G_c$ applied to the LR model cell and a time-varying coupling current of $Z_1 * (V_2 - V_1) * G_c$ applied to the real GP ventricular cell, where V_1 and V_2 are the time-varying membrane potentials of the real GP ventricular cell and the LR model cell, respectively. This produces an effective increase in the size (as represented by an increase in the current threshold and a decrease in the input resistance) of cell 1 by a factor of $1/Z_1$ and of cell 2 by a factor of $1/Z_2$. In our experiments we have normalized the size of each of the real cells studied by using a factor of Z_1 for each real GP ventricular cell, such that its effective current threshold with current pulses of 2 ms duration is equal to that of the standard size LR model cell (2.6 nA).

RESULTS

Fig. 1 illustrates recordings from a GP ventricular cell (*solid line*) and a simultaneous real-time computation of the LR ventricular cell model (*dotted line*), with repetitive 1-Hz direct stimulation of the real cell with current pulses of 2 ms duration. For this cell the current threshold was 1.8 nA and the input resistance was 20.7 MΩ before size normalization. We used a Z_1 factor of 0.69 (1.8/2.6, see Materials and Methods) for the coupling current applied to the real cell to normalize the size of the real cell to that of the LR model cell. This resulted in an effective current threshold of 2.6 nA and an input resistance of 14.3 MΩ for the real cell during this experiment. A similar procedure was used for all of the real GP ventricular cells we studied, with all data obtained after normalization of the size of the real GP ventricular cell (the leader cell) to a current threshold of 2.6 nA. For Fig. 1, we used a coupling protocol in which the GP ventricular cell was not initially coupled to the LR model cell. A G_c of 10 nS was established for the period marked by the horizontal arrow in Fig. 1, *A* and *C*. The second stimulated action potential of each trace occurs during the period of coupling and propagates to the LR model cell. During the time period after activation of the leader cell and before activation of the follower cell, there is a prominent partial repolarization of the membrane potential of the leader cell due to the current flow out of the leader cell and into the follower cell. Fig. 1 *B* shows the coupling current recorded simultaneously with the voltage recordings of Fig. 1 *A*, which was recorded in the control external solution. Positive coupling current is in the direction from the real cell to the model cell. Fig. 1, *C* and *D*, shows recordings from the same cell after the addition of 1 μM nifedipine to the external solution, again with a protocol of no coupling during the initial portion of the trace and then a G_c of 10 nS. Nifedipine shortened the action potential of the GP ventricular cell, when uncoupled, and caused a greater partial repolarization of the GP ventricular cell and a greater conduction delay during the conduction process after coupling had been established.

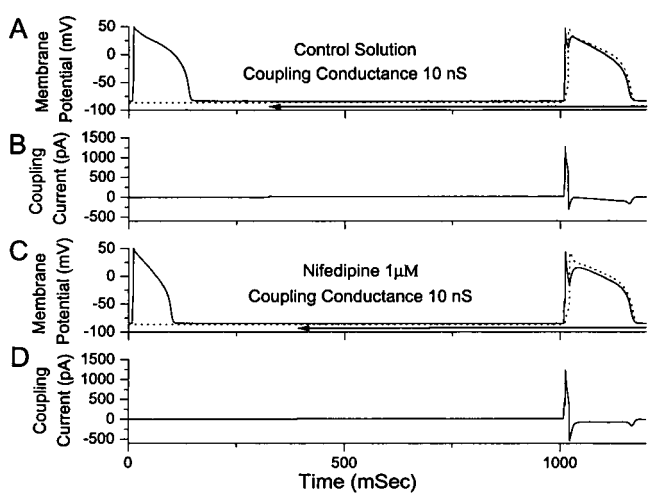

FIGURE 1 (*A*) Recording from a guinea pig ventricular cell (——) and a simultaneous real-time computation of the LR ventricular cell model (– – –), with repetitive 1-Hz direct stimulation of the real cell with current pulses of 2 ms duration. For the period of recording shown here, the model is initially not coupled to the real cell, and coupling is established at G_c = 10 nS during the period marked by the horizontal arrow. The second stimulated action propagates to the LR model cell. (*B*) Coupling current recorded simultaneously with the voltage recordings of *A*. Positive coupling current is in the direction from the real cell to the model cell. (*C* and *D*) Recordings from the same cell after the addition of 1 μM nifedipine to the external solution. Cell R090595D, records D01 and D22.

For this same hybrid cell pair (GP ventricular cell coupled to a LR model cell) we recorded action potential conduction from the GP ventricular cell to the LR model cell over a wide range of values of G_c. Fig. 2 *A* shows recording from a GP ventricular cell (*solid line*) and a simultaneous real-time computation of the LR model cell (*dotted line*), with repetitive 1-Hz direct stimulation of the real cell with current pulses of 2 ms duration. Values of G_c of 50, 30, 20, 15, 10, 8, 7, and 6 nS are indicated by the letters *a*, *b*, *c*, *d*, *e*, *f*, *g*, and *h*, respectively, on the dotted traces, which are the solutions for the LR model cell. Fig. 2 *B* shows the coupling currents recorded simultaneously with the voltage recordings of the top panel. For the largest value of G_c used (50 nS, trace a) the conduction delay is only 1 ms. As G_c was decreased, the conduction delay increased and the slope of the initial partial repolarization of the leader cell and the peak magnitude of the coupling current decreased. For the smallest value of G_c that allowed successful conduction (7 nS, trace g), the conduction delay was 21 ms. For each value of G_c for which conduction was successful, the leader cell (GP ventricular cell) shows a partial repolarization during the conduction process, then depolarizes

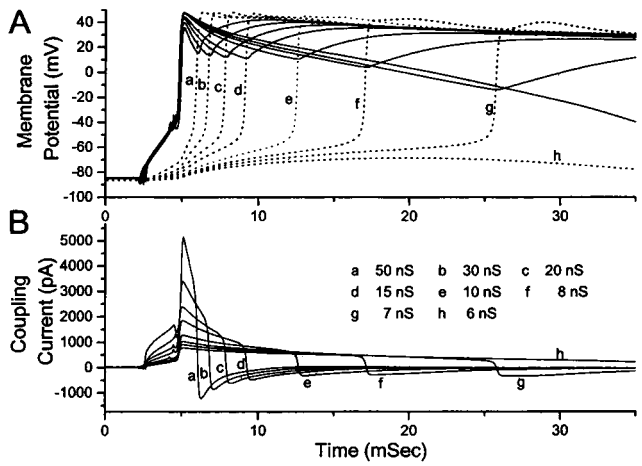

FIGURE 2 (*A*) Recording from a guinea pig ventricular cell (——) and a simultaneous real-time computation of the LR ventricular cell model (– – –), with repetitive 1-Hz direct stimulation of the real cell with current pulses of 2 ms duration. Recordings are from the same cell as for Fig. 1, but at a faster sweep speed, with results for various values of G_c displayed. Values of G_c of 50, 30, 20, 15, 10, 8, 7, and 6 nS are indicated by the letters *a*, *b*, *c*, *d*, *e*, *f*, *g*, and *h*, respectively, on the dotted traces, which are the solutions for the LR model cell. (*B*) Coupling current recorded simultaneously with the voltage recordings of *A*. Positive coupling current is in the direction from the real cell to the model cell. Cell R090595D, records D01, D02, D03, D04, D07, D08, D09, and D10.

again after the activation of the follower cell (the LR model cell). With smaller values of G_c (and longer conduction delays) this secondary depolarization of the leader cell occurs with a slower time course.

Fig. 3 shows the effect of nifedipine (1 μM) on conduction delay (shown in Fig. 3 *A*) between the real GP ventricular cell (same cell as for Figs. 1 and 2) and the LR model cell as a function of G_c in control and 1 μM nifedipine solution. For larger values of G_c there is only a short conduction delay, and this delay is not affected by the addition of nifedipine. As G_c was decreased there was not only an increase in the conduction delay in the control solution, but also an increased effect of the nifedipine solution. This effect is illustrated in Fig. 3 *B*, which shows action potential conduction from the GP ventricular cell (*solid lines*) to the LR model cell (*dotted lines*) in control solution (C) and in 1 μM nifedipine solution (NIF) with a G_c of 10 nS. The upstrokes of the two real cell recordings (from the same cell) have been aligned in time for clarity of presentation. Conduction in the NIF solution has a longer delay and a larger early repolarization of the real cell. Note that the action potential peak amplitude of the real cell is minimally affected by nifedipine. At G_c values below 10 nS, there is a very substantial effect of the nifedipine solution. Conduction failure occurred for a G_c less than 7 nS in the control solution (see Fig. 2), but occurred for a G_c less than 9 nS in the nifedipine solution (data not shown).

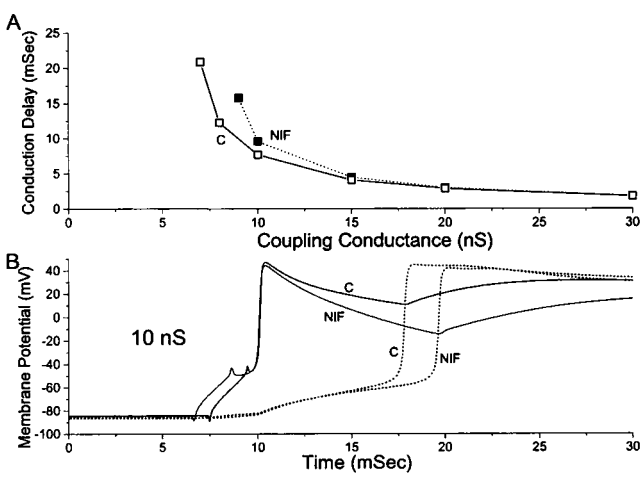

FIGURE 3 (*A*) Plot of the conduction delay between the real GP ventricular cell (same cell as for Figs. 1 and 2) and the LR model cell as a function of G_c in control and 1 μM nifedipine solution. (*B*) Action potential conduction from the GP ventricular cell to the LR model cell in control solution (C) and in 1 μM nifedipine solution (NIF) with a G_c of 10 nS. Recordings from the real cell are solid lines, and the computed results for the LR model cell are dotted lines. The upstrokes of the two real cell recordings have been aligned in time for clarity of presentation.

In addition to the effects of G_c, the relative sizes of the two cells of a cell pair can also strongly affect the conduction delay between the cells. Fig. 4 illustrates this phenomenon from a hybrid cell pair in which the leader cell (with direct stimulation through the pipette) is a GP ventricular cell and the follower cell is the LR model cell. For this cell

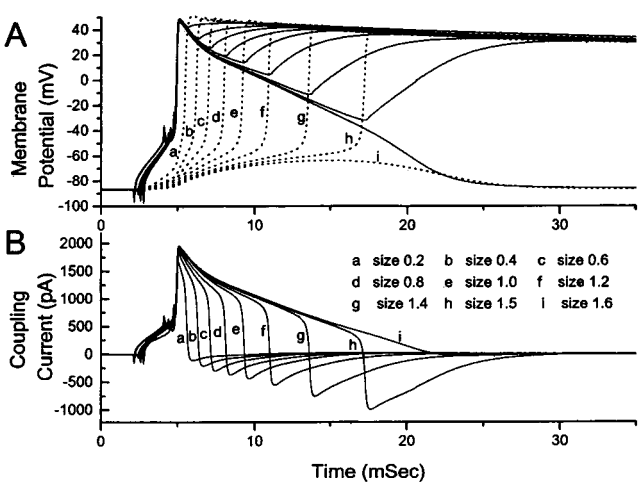

FIGURE 4 (*A*) Recording from a guinea pig ventricular cell (——) and a simultaneous real-time computation of the LR model cell model (– – –), with repetitive 1-Hz direct stimulation of the real cell with current pulses of 2 ms duration. We adjusted the size of the real cell to be the same as the size of the standard LR model cell. We then repetitively stimulated the GP ventricular cell, using a G_c of 15 nS, while varying the size of the LR model cell from 0.2 to 2.0 with respect to a standard size of 1.0. Recordings are shown for various values of the size of the LR model cell with sizes of 0.2, 0.4, 0.6, 0.8, 1.0, 1.2, 1.4, 1.5, and 1.6 indicated by the letters *a*, *b*, *c*, *d*, *e*, *f*, *g*, *h*, and *i*, respectively, on the dotted traces, which are the solutions for the LR model cell. (*B*) Coupling current recorded simultaneously with the voltage recordings of *A*. Positive coupling current is in the direction from the real cell to the model cell. Cell R090695A, records A12, A13, A14, A15, A16, A17, A18, A19, and A20.

the current threshold was 2.9 nA before size normalization, so we used a Z_1 factor of 1.12 (2.9/2.6) for the coupling current applied to the real cell to normalize the size of the real cell to that of the standard LR model cell. Fig. 4 *A* shows recordings from the real cell (*solid line*) and the LR model cell (*dotted line*), with repetitive 1-Hz direct stimulation of the real cell. With a size factor of 1.0 for the LR model cell, we found the critical value of G_c below which conduction failed to be 7.0 nS. We then repetitively stimulated the GP ventricular cell, using a G_c of 15 nS, while varying the size of the LR model cell from 0.2 up to a value that produced conduction failure from the GP ventricular cell to the LR model cell. Fig. 4 *A* shows recordings for various values of the size of the LR model cell, with sizes of 0.2, 0.4, 0.6, 0.8, 1.0, 1.2, 1.4, 1.5, and 1.6 indicated by the letters *a*, *b*, *c*, *d*, *e*, *f*, *g*, *h*, and *i*, respectively, on the dotted traces, which are the solutions for the LR model cell. Fig. 4 *B* shows the coupling current recorded simultaneously with the voltage recordings of the top panel. Note that the process of increasing the size of the follower cell produces increases in conduction delay that can lead to conduction failure, just as decreasing the coupling conductance between the two cells (compare Fig. 4 to Fig. 2). However, the actual modulation of the action potential shape of the leader cell and the time course and magnitude of the coupling current are quite different for the two methods of increasing conduction delay. For decreases in G_c (Fig. 2), the slope of the early repolarization during the conduction process becomes progressively less steep for the leader cell and the peak magnitude of the coupling current becomes smaller. For increases in the size of the follower cell, without changing the size of the leader cell or G_c (Fig. 4), the slope of the early repolarization during the conduction process remains the same and the peak magnitude of the coupling current remains nearly constant, but the extent of partial repolarization of the real cell increases.

Even though the data for changing coupling conductance (Fig. 2) and for changing the size of the follower cell (Fig. 4) were obtained by using real isolated cells from different preparations, each of these real cells was coupled to a standard LR model cell, allowing us to compare these two different methods of altering conduction delay in terms of the charge transferred to the follower cell to produce excitation. For each of the coupling current traces shown in Figs. 2 and 4, we integrated the coupling current (pA) as applied to the follower cell, starting at the time of the beginning of the 2-ms-duration stimulus to the leader cell and ending at the time at which the potential of the follower cell crosses zero voltage. Fig. 5 *A* shows (*solid squares connected by a solid line*) the coupling current integral (pC) for the results of Fig. 2, for which we varied the coupling conductance from 50 nS to 7 nS, plotted against the conduction delay (the time delay from the zero crossing of the leader cell to the zero crossing of the follower cell). As the conduction delay is increased (associated with decreases in the coupling conductance), the coupling current integral remains nearly constant until the conduction delay exceeds

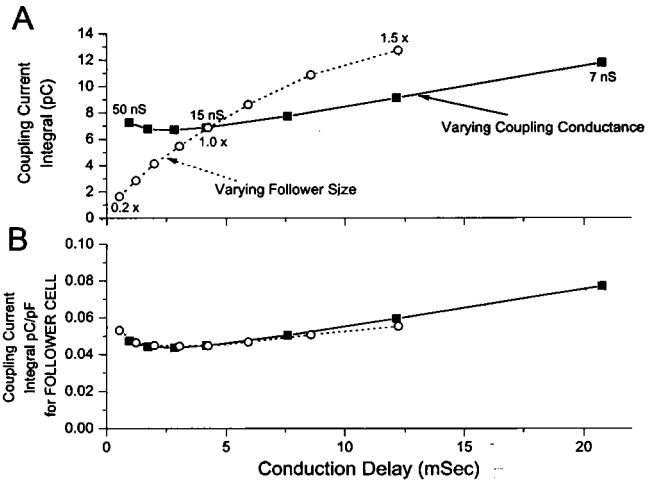

FIGURE 5 Time integral of coupling current during the conduction process as a function of conduction time as either the coupling conductance (■, integrated data from Fig. 2 *B*) or the relative size of the follower cell (○, integrated data from Fig. 4 *B*) is varied. For *A* the integral is expressed simply as a time integral of current (pC), whereas for *B* the results of *A* are replotted and scaled by the capacitance of the follower cell (the LR model, 153.4 pF multiplied by the size factor for the follower cell).

5 ms and then progressively increases. Fig. 5 *A* also shows (*open circles connected by a dotted line*) the coupling current integral for the results of Fig. 4, for which we varied the effective size of the follower cell from 0.2 to 1.5 times the standard size. As the conduction delay is increased (associated with increases in the relative size of the follower cell) there is a large increase in the coupling current integral, representing the increasing demand of the larger follower cell for charge to achieve a threshold voltage. Note that the two curves in Fig. 5 *A* intersect for a coupling conductance of 15 nS and a size factor of 1.0, which is expected, because we used a coupling conductance of 15 nS when varying the size of the follower cell (Fig. 4) and we used a size factor of 1.0 while varying the coupling conductance (Fig. 2). In Fig. 5 *B* we have replotted the data of Fig. 5 *A* with a normalization of the coupling current integral to the effective capacitance of the follower cell. Because the standard size LR model cell has 153.4 pF, this process simply divides the coupling current integral by 153.4 pF times the size factor for the follower cell. The data for varying the coupling conductance (*solid squares*) have the same relationship to conduction delay as shown in Fig. 5 *A*, whereas the data for varying the size of the follower cell (*open circles*) are now nearly superimposable over the data for varying the coupling conductance.

We also found that changing the relative size of the model cell (follower cell) with respect to the real cell (leader cell) modulated the effects of drugs on the conduction process. In Fig. 6 we show results for three hybrid cell pairs, each consisting of a real GP ventricular cell coupled to the LR model cell. In each part of the figure we show results for conduction delay (milliseconds) as a function of the relative size of the model cell for control (C) solution, the applica-

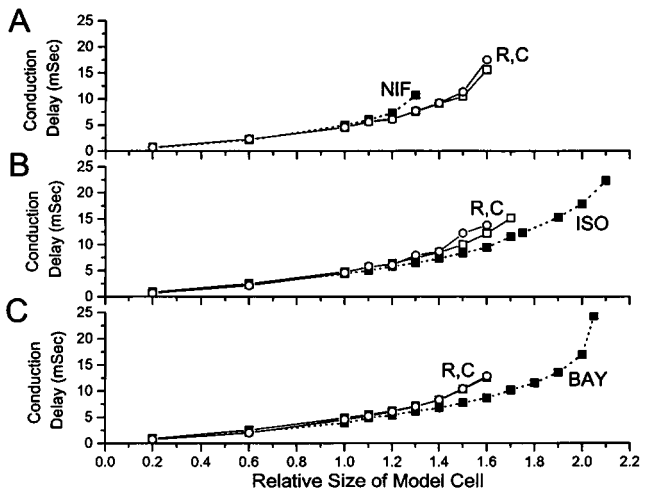

FIGURE 6 Each part of the figure shows results for conduction delay (ms) as a function of the relative size of the model cell for control (C) solution, the application of a drug, and then in the return to the control solution (R), when G_c is fixed at 15 nS. For each part the data from the control solution are plotted as open squares, the data from the drug solution are plotted as filled squares, and the data from the recovery solution are plotted as open squares. (*A*) Effects of 1 μM nifedipine; (*B*) effects of 20 nM isoproterenol; (*C*) effects of 1 μM BayK 8644. Cells R110695A, R110395F, and R110695B were used for *A*, *B*, and *C*, respectively.

tion of a drug, and then in the return to the control solution (R) when the coupling conductance is fixed at 15 nS. For each part of the figure, the data in the control solution are plotted as open squares, the data in the drug solution are plotted as filled squares, and the data in the recovery solution are plotted as open circles. Fig. 6 *A* illustrates the effects of 1 μM nifedipine. In the control solution, conduction failure occurred for a relative size of model cell greater than 1.6, whereas in the nifedipine solution, conduction failure occurred for a relative size of model cell greater than 1.3. After washout of the nifedipine solution, conduction failure again occurred for a relative size of model cell greater than 1.6. Nifedipine (which partially blocks the L-type calcium current) decreased the critical relative size of the model (follower) cell for successful conduction and increased the critical conductance for successful conduction between cells of a cell pair (Fig. 3). These results suggested that the effects of agents that increase calcium current would be to increase the critical relative size of the model (follower) cell above that at which conduction would fail, as well as to decrease the value of G_c to a level below which conduction would fail. Fig. 6 *B* illustrates the effects of 20 nM isoproterenol (ISO). The maximum value of the relative size of the model (follower) cell for successful conduction between cells of a cell pair coupled by 15 nS was increased from 1.7 to 2.1 by isoproterenol, and this effect was reversible upon washout of the isoproterenol. Fig. 6 *C* illustrates the effects of 1 μM BayK 8644 (BAY). The maximum value of the relative size of the model cell for successful conduction between cells of a cell pair was increased from 1.6 to 2.15 by the BayK 8644, and this effect was reversible upon washout of the BayK 8644.

Fig. 7 illustrates the effects of nifedipine and isoproterenol applied separately to a GP ventricular cell when this real cell was the leader cell of a hybrid cell pair for which the follower cell was the LR model cell. For this cell pair, after the size of the real cell was normalized, the critical G_c for successful conduction was 6.6 nS. Fig. 7 illustrates results obtained with a G_c of 6.6 nS. The three traces for the real cell (*solid lines*) and the model cell (*dotted lines*) labeled as CONTROLS were recorded during the initial control period, after the washout of the isoproterenol solution, and after the washout of the nifedipine solution, respectively. Each of these pairs of recordings shows a conduction delay of 21–22 ms. When we applied 20 nM isoproterenol, the critical value of G_c was reduced to 4.5 nS. For a G_c of 6.6 nS, as shown by the set of traces labeled ISO, the conduction delay was decreased from the control conditions (22 ms) to 14 ms. Note that the early repolarization of the leader cell (real GP ventricular myocyte) is less in the ISO solution than in the control solution. This effect of 20 nM isoproterenol was also completely reversible, as shown by the CONTROLS recordings. When we then applied the 1 μM nifedipine solution to the same cell, after the recovery from the isoproterenol effects, the critical G_c was increased to 8.5 nS, with the pair of curves labeled NIF showing conduction failure with a G_c of 6.6 nS. The conduction failure produced by nifedipine at this value of G_c was completely reversible, as shown by the nearly identical three sets of recordings made in the control solution. Note that the early repolarization of the action potential in the leader cell (real GP ventricular myocyte) occurs at a more rapid rate in the NIF solution than in the control solution. Fig. 7 *B* shows the

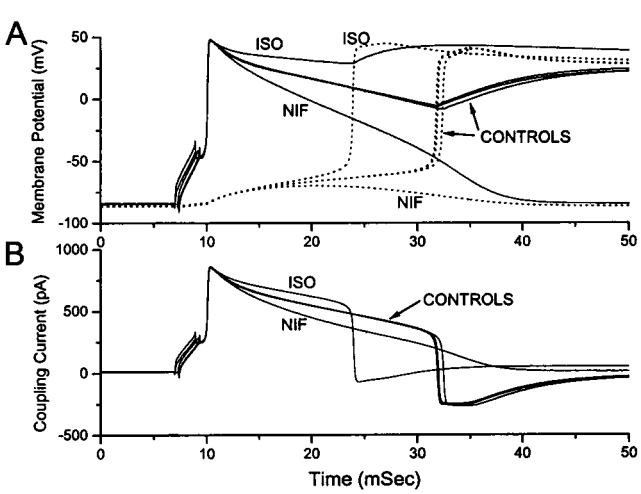

FIGURE 7 (*A*) Effects of 20 nM isoproterenol (ISO) and the effects of 1 μM nifedipine (NIF) on conduction between a GP ventricular cell and the LR model cell. For this cell, in control solution, conduction block occurred for G_c less than 6.6 nS. In *A* results are illustrated for a G_c of 6.6 nS for the initial control, the washout after ISO, and the washout after NIF (CONTROLS), as well as the response to ISO and to NIF. Recordings from the real cell are shown as solid lines, and the simultaneously simulated model responses are shown as dotted lines. (*B*) Simultaneously recorded coupling currents for the recordings of *A*. Cell R102795A.

simultaneously recorded coupling currents for the recordings of Fig. 7 *A*. In the ISO solution the peak amplitude of coupling current is unchanged, but the magnitude of the coupling current is maintained at a higher level during the conduction process (because of the higher level of membrane potential of the leader cell; see Fig. 7 *A*), and thus the follower cell reaches the voltage threshold for activation sooner than in the control solution. For the NIF solution, the peak amplitude of the coupling current is also equal to that recorded in the control solution, but the amplitude of the coupling current declines more rapidly in the NIF solution than in the control solution. Because, for G_c of 6.6 nS, this hybrid cell pair had conduction failure in the NIF solution, the coupling current flow in the NIF solution does not have a reversal of polarity (because the follower cell never activates) and declines progressively toward zero. In the control recordings and in the ISO recording, there is a rapid reversal in the polarity of the coupling current as activation of the follower cell (the LR model cell) occurs.

In Fig. 8 we show a extension of the results of Fig. 7 to a statistical comparison of the effects of 20 nM isoproterenol (ISO) and 1 μM nifedipine (NIF) on the critical G_c, below which an action potential fails to propagate from an isolated GP ventricular cell to the LR model when the size of the GP ventricular cell has been adjusted to equal that of the standard LR model cell (current threshold 2.6 nA for a 2-ms-duration pulse). For each cell tested, except for the cell used for the illustration of Fig. 6, we used either ISO (on seven additional cells) or NIF (on eight additional cells) as a test solution, but not both. For these experiments we determined the critical G_c in the control solution and then switched to either ISO or NIF and again determined the critical G_c. Control values of the critical G_c for the eight cells treated with ISO were 6.9 ± 0.1 nS and control values of the critical G_c for the nine cells treated with NIF were 6.7 ± 0.1 nS. The critical G_c was significantly decreased from control values by 20 nM isoproterenol (5.3 ± 0.2 nS, n = 8, $p < 0.001$) and was significantly increased by 1 μM nifedipine (8.8 ± 0.2 nS, n = 9, $p < 0.0001$) (mean ± SEM, statistical evaluation by paired t-test, comparing control versus test values for each group of cells).

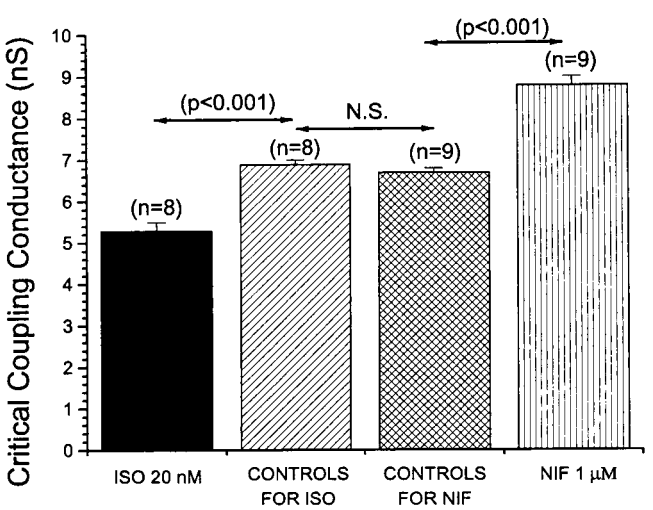

FIGURE 8 Comparison of effects of 20 nM isoproterenol (ISO) and 1 μM nifedipine (NIF) on the critical G_c below which action propagation fails from an isolated GP ventricular cell to the LR model cell when the size of the GP ventricular cell has been adjusted to equal that of the standard LR model cell (current threshold, 2.6 nA for a 2-ms duration pulse).

DISCUSSION

We have created hybrid cell pairs in which one cell is a real guinea pig ventricular myocyte and the other cell is a real-time simulation of the LR model (Luo and Rudy, 1994a,b), to systematically evaluate the effects of changes in coupling conductance, changes in the magnitude of the L-type calcium current, and changes in the relative sizes of the leader and the follower cell. For all of these experiments, we have used the LR model cell as the "follower" cell of the cell pair and the real GP ventricular cell as the "leader" of the cell pair. For all of the pharmacological interventions, the drugs were applied directly to the bath, thus affecting the real GP ventricular cell, without any changes in the LR model cell equations to attempt to simulate corresponding changes in the magnitude of the L-type calcium current of the LR model cell. We were thus able to consistently and reversibly create specific asymmetric conditions in cell membrane properties for the two cells of the cell pair. Nifedipine has a very specific action of blocking L-type calcium currents, and the concentration of NIF with the half-maximum effect on calcium current was 1.4 μM in the guinea pig papillary muscle (Kohlhardt and Fleckenstein, 1977).

We are using the cell pair model as a simplified form of the complex, discontinuous conduction that has been observed in cardiac tissue after myocardial ischemia and which is thought to contribute to the genesis of cardiac arrhythmias. In the healed myocardial infarction, the resting membrane potential has returned to nearly normal values (Ursell et al., 1985; Gardner et al., 1985), although the membrane properties of the surviving cells may be abnormal, with decreased transient outward current (Lue and Boyden, 1992; Jeck et al., 1995) and decreased L-type calcium current and sodium current (Boyden and Pinto, 1994; Lue and Boyden, 1992). The effective conduction velocity becomes very slow and is characterized as discontinuous conduction with a very irregular ("zig-zag") spatial pattern instead of the uniform anisotropic pattern of normal ventricular tissue (de Bakker et al., 1993). Fractionated electrograms consisting of two or more discrete deflections were recorded in preparations from healed infarctions (Gardner et al., 1985; Ursell et al., 1985), which is further evidence of discontinuous conduction. Action potentials in these regions have prepotentials, and notches on the depolarization and repolarization phase due to electrotonic interactions with nearby cells (Kienzle et al., 1987). Zuanetti et

al. (1990) showed that slow conduction by a premature stimulus in the epicardial tissue of a healed infarct was modulated by β-stimulation with isoproterenol. Although isoproterenol did not change the activation pattern and velocity for stimulations at the basic drive frequency, for premature stimulations it reduced the slowing of conduction, changed the conduction pattern, and prevented the occurrence of functional block in tissues. Around the region of conduction block they recorded fractionated electograms, indicative of slow, discontinuous conduction. Previous reports (El Sherif, 1978; Gilmour et al., 1983) also suggested that catecholamines may improve conduction velocity and reverse abnormalities in conduction after infarction. However, isoproterenol, in addition to its well-known effects on increasing I_{Ca} (Tsien, 1977; Drummond and Severson, 1979), has many effects on cardiac tissues, such as an increase or decrease in sodium current (Gillis and Kohlhardt, 1988; Ono et al., 1989; Schubert et al., 1990) and an increase in chloride current (Harvey and Hume, 1989; Bahinski et al., 1989), delayed rectifier potassium current (Bennett and Begenisich, 1987; Matsuura et al., 1987; Walsh et al., 1988; Yazawa and Kameyama, 1990), and intracellular sodium concentration (Wilde and Kleber, 1991). Another possible action of isoproterenol might be a modulation of gap junctional conductance by cAMP-mediated phosphorylation (De Mello and van Loon, 1987).

We have demonstrated that significant delays in action potential conduction for a cell pair can occur either with a decreased value of coupling conductance (Fig. 2) or with an asymmetry in size (Fig. 4) such that the follower cell is larger than the leader cell. As the conduction delay is increased, the effects of the intervention on the coupling current are quite different for the two conditions. For an increasing delay produced by a decreasing value of coupling conductance, the peak value of coupling current during the propagation process becomes progressively smaller as the current flow is more limited by the coupling conductance. For an increasing delay produced by an increasing value of size for the follower cell, the peak value of coupling current remains nearly constant. We have shown that isoproterenol, at very low concentrations, can reversibly decrease the critical coupling conductance for a cell pair with fixed cell sizes, or, for a fixed value of coupling conductance, increase the maximum allowable asymmetry in cell size for successful conduction. For either of these effects, we were able to show that treatment with BayK 8644, which more specifically increases the magnitude of the L-type calcium current, was able to mimic the actions of isoproterenol. Treatment of the leader cell of the cell pair with nifedipine, which selectively lowers the magnitude of the L-type calcium current, had effects opposite those of isoproterenol or BayK 8644. The actions of nifedipine, isoproterenol, and BayK 8644 are all limited to conditions in which the conduction delay is on the order of 5 ms or more, whether this delay is caused by limited coupling conductance or by asymmetry in size of the cells. This limitation is consistent with the time course of the L-type calcium current and suggests that the effects of calcium channel blockers or β-adrenergic blocking drugs, in addition to being selective for regions of the heart that depend on the L-type calcium current for the upstroke of the action potential, would also be somewhat selective for regions of the heart that have discontinuous conduction, either normally or because of some pathological condition.

REFERENCES

Bahinski, A., A. C. Nairn, P. Greengard, and D. C. Gadsby. 1989. Chloride conductance regulated by cyclic AMP-dependent protein kinase in cardiac myocytes. *Nature.* 340:718–721.

Beeler, G. W., and H. Reuter. 1977. Reconstruction of the action potential of ventricular myocardial fibres. *J. Physiol. (Lond.).* 268:177–210.

Bennett, P. B., and T. B. Begenisich. 1987. Catecholamines modulate the delayed rectifying potassium current (IK) in guinea pig ventricular myocytes. *Pflugers Arch.* 410:217–219.

Boyden, P. A., and J. M. Pinto. 1994. Reduced calcium currents in subendocardial Purkinje myocytes that survive in the 24- and 48-hour infarcted heart. *Circulation.* 89:2747–2759.

de Bakker, J. M., F. J. van Capelle, M. J. Janse, S. Tasseron, J. T. Vermeulen, N. de Jonge, and J. R. Lahpor. 1993. Slow conduction in the infarcted human heart. "Zigzag" course of activation. *Circulation.* 88: 915–926.

De Mello, W. C., and P. van Loon. 1987. Further studies on the influence of cyclic nucleotides on junctional permeability in heart. *J. Mol. Cell. Cardiol.* 19:763–771.

Drummond, G. I., and D. L. Severson. 1979. Cyclic nucleotides and cardiac function. *Circ. Res.* 44:145–153.

El Sherif, N. 1978. Reentrant ventricular arrhythmias in the late myocardial infarction period. 6. Effect of the autonomic system. *Circulation.* 58: 103–110.

Gardner, P. I., P. C. Ursell, J. J. Fenoglio, and A. L. Wit. 1985. Electrophysiologic and anatomic basis for fractionated electrograms recorded from healed myocardial infarcts. *Circulation.* 72:596–611.

Gillis, A. M., and M. Kohlhardt. 1988. Voltage-dependent V_{max} blockade in Na^+-dependent action potentials after beta 1- and H2-receptor stimulation in mammalian ventricular myocardium. *Can. J. Physiol. Pharmacol.* 66:1291–1296.

Gilmour, R. F., J. J. Heger, E. N. Prystowsky, and D. P. Zipes. 1983. Cellular electrophysiologic abnormalities of diseased human ventricular myocardium. *Am. J. Cardiol.* 51:137–144.

Harvey, R. D., and J. R. Hume. 1989. Autonomic regulation of a chloride current in heart. *Science.* 244:983–985.

Jeck, C. D., J. M. Pinto, and P. A. Boyden. 1995. Transient outward currents in subendocardial Purkinje myocytes surviving in the infarcted heart. *Circulation.* 92:465–473.

Joyner, R. W. 1986. Modulation of repolarization by electrotonic interactions. *Jpn. Heart J.* 27:167–183.

Joyner, R. W., H. Sugiura, and R. C. Tan. 1991. Unidirectional block between isolated rabbit ventricular cells coupled by a variable resistance. *Biophys. J.* 60:1038–1045.

Kienzle, M. G., R. C. Tan, B. M. Ramza, M. L. Young, and R. W. Joyner. 1987. Alterations in endocardial activation of the canine papillary muscle early and late after myocardial infarction. *Circulation* 76:860–874.

Kohlhardt, M., and A. Fleckenstein. 1977. Inhibition of the slow inward current by nifedipine in mammalian ventricular myocardium. *Naunyn Schmiedebergs Arch. Pharmacol.* 298:267–272.

Kumar, R., and R. W. Joyner. 1995. Calcium currents of ventricular cell pairs during action potential conduction. *Am. J. Physiol.* 268: H2476–H2486.

Lue, W. M., and P. A. Boyden. 1992. Abnormal electrical properties of myocytes from chronically infarcted canine heart. Alterations in V_{max} and the transient outward current. *Circulation.* 85:1175–1188.

Luo, C. H., and Y. Rudy. 1991. A model of the ventricular cardiac action potential. Depolarization, repolarization, and their interaction. *Circ. Res.* 68:1501–1526.

Luo, C. H., and Y. Rudy. 1994a. A dynamic model of the cardiac ventricular action potential. I. simulations of ionic currents and concentration changes. *Circ. Res.* 74:1071–1096.

Luo, C. H., and Y. Rudy. 1994b. A dynamic model of the cardiac ventricular action potential. II. afterdepolarizations, triggered activity, and potentiation. *Circ. Res.* 74:1097–1113.

Matsuura, H., T. Ehara, and Y. Imoto. 1987. An analysis of the delayed outward current in single ventricular cells of the guinea-pig. *Pflugers Arch.* 410:596–603.

Ono, K., T. Kiyosue, and M. Arita. 1989. Isoproterenol, DBcAMP, and forskolin inhibit cardiac sodium current. *Am. J. Physiol.* 256: C1131–C1137.

Schubert, B., A. M. J. VanDongen, G. E. Kirsch, and A. M. Brown. 1990. Inhibition of cardiac Na^+ currents by isoproterenol. *Am. J. Physiol.* 258:H977–H982.

Sugiura, H., and R. W. Joyner. 1992. Action potential conduction between guinea pig ventricular cells can be modulated by calcium current. *Am. J. Physiol.* 263:H1591–H1604.

Tan, R. C., and R. W. Joyner. 1990. Electrotonic influences on action potentials from isolated ventricular cells. *Circ. Res.* 67:1071–1081.

Tsien, R. W. 1977. Cyclic AMP and contractile activity in heart. *Adv. Cyclic Nucleotide Res.* 8:363–420.

Ursell, P. C., P. I. Gardner, A. Albala, J. J. Fenoglio, and A. L. Wit. 1985. Structural and electrophysiological changes in the epicardial border zone of canine myocardial infarcts during infarct healing. *Circ. Res.* 56: 436–451.

Walsh, K. B., T. B. Begenisich, and R. S. Kass. 1988. Beta-adrenergic modulation in the heart. Independent regulation of K and Ca channels. *Pflugers Arch.* 411:232–234.

Wilde, A. A., and A. G. Kleber. 1991. Effect of norepinephrine and heart rate on intracellular sodium activity and membrane potential in beating guinea pig ventricular muscle. *Circ. Res.* 68:1482–1489.

Wilders, R., R. Kumar, R. W. Joyner, H. J. Jongsma, E. E. Verheijck, D. Golod, A. C. G. Van Ginneken, and W. N. Goolsby. 1996. Action potential conduction between a ventricular cell model and an isolated ventricular cell. *Biophys. J.* 70:281–295.

Yazawa, K., M. Kaibara, M. Ohara, and M. Kameyama. 1990. An improved method for isolating cardiac myocytes useful for patch-clamp studies. *Jpn. J Physiol.* 40:157–163.

Yazawa, K., and M. Kameyama. 1990. Mechanism of receptor-mediated modulation of the delayed outward potassium current in guinea-pig ventricular myocytes. *J. Physiol. (Lond.).* 421:135–150.

Zuanetti, G., R. H. Hoyt, and P. B. Corr. 1990. Beta-adrenergic-mediated influences on microscopic conduction in epicardial regions overlying infarcted myocardium. *Circ. Res.* 67:284–302.